The Role of L1 in Axon Pathfinding and Fasciculation

A.E. Wiencken-Barger[1,5], J. Mavity-Hudson[1], U. Bartsch[2,6], M. Schachner[2] and V.A. Casagrande[1,3,4]

[1]Department of Cell and Developmental Biology, Vanderbilt University, Nashville, TN, USA, [2]Zentrum für Molekulare Neurobiologie, Universität Hamburg, Germany, [3]Department of Psychology, Vanderbilt University, Nashville, TN, USA and [4]Department of Ophthalmology and Visual Sciences, Vanderbilt University, Nashville, TN, USA
[5]Current address: Department of Cellular Biochemistry and Biophysics, Memorial Sloan-Kettering Cancer Institute, New York, USA
[6]Current address: Transplantationslabor, Klinik und Poliklinik für Augenheilkunde, Universitätsklinikum Hamburg-Eppendorf, Germany

The neural cell adhesion molecule L1 has been found to play important roles in axon growth and fasciculation. Our main objective was to determine the role of L1 during the development of connections between thalamus and cortex. We find that thalamocortical and corticothalamic axons in mice lacking L1 are hyperfasciculated, a subset of thalamocortical axons make pathfinding errors and thalamocortical axon growth cones are abnormally long in the subplate. These defects occur despite formation of six cortical layers and formation of topographically appropriate thalamocortical connections. The loss of L1 is accompanied by loss of expression of ankyrin-B, an intracellular L1 binding partner, suggesting that L1 is involved in the regulation of Ank2 stability. We postulate that the pathfinding errors, growth cone abnormalities and hyperfasciculation of axons following loss of L1 reflect both a shift in binding partners among axons and different substrates and a loss of appropriate interactions with the cytoskeleton.

Keywords: ankyrin-B, cell adhesion, cortex, cytoskeleton, growth cone, thalamus

Introduction

Axon guidance during development involves a formidably complex set of mechanisms that can be divided broadly into four major categories: chemoattraction and repulsion, and contact attraction and repulsion (Tessier-Lavigne and Goodman, 1996). These mechanisms are coordinated to direct axons to their proper locations and may involve dozens of molecules applying different forces. The common steps in axon guidance include initial outgrowth and formation of a growth cone, axon bundling or fasciculation, defasciculation, branching, target acquisition, synaptogenesis, and maintenance of the synapse. Neural cell adhesion molecules (CAMs) of the immunoglobulin superfamily are involved in many of these events. In mammals, one of the best known of these CAMs is L1 (Crossin and Krushel, 2000). L1 is a member of a large subfamily of molecules that includes Nr-CAM, Ng-CAM, neurofascin, neuroglian, aBGP and CHL1 (Moos et al., 1988). L1 is promiscuous, with many binding partners, including but not limited to itself, integrins, NCAM, TAG-1/axonin-1, contactin/F3/F11, extracellular matrix molecules and ankyrin in the cytoplasmic domain (Grumet, 1992; Grumet et al., 1996; Hortsch, 1996; Brummendorf et al., 1998; Needham et al.,

2001). Analysis of the structure, function and signaling pathways related to L1 has suggested that this CAM plays a variety of important roles in neural development and in learning and memory in adult animals (for reviews, see Walsh and Doherty, 1997; Brummendorf et al., 1998).

A role for L1 in axon pathfinding is most strongly supported by data from animals that are missing the molecule. Mutations in the gene for L1 lead to a condition in humans known as L1 disease. Patients with the disorder have mental retardation, hydrocephalus of varying severity and problems with peripheral limb movements (Fransen et al., 1997). In part, this phenotype is due to defects in major axonal tracts, such as the corticospinal tract and the corpus callosum. One of the first discoveries about L1 mutant mice was that they show hypoplasia of the corticospinal tract due to pathfinding errors: corticospinal axons fail to cross the midline at the decussation (Cohen et al., 1997; Dahme et al., 1997). Additionally, L1 mutants variably exhibit hypotrophy or agenesis of the corpus callosum (Demyanenko et al., 1999). Mutations are found throughout the L1 molecule in L1 disease patients. Interestingly, the position of the mutation relates to the phenotype of the disease. For instance, cytoplasmic mutations tend to cause axon pathfinding errors, but rarely cause hydrocephalus (Yamasaki et al., 1997). This finding suggests that the intracellular domain of L1 functions in some aspect of axonal tract formation or maintenance.

Located just underneath the cell membrane is a network of cytoskeletal elements composed of several proteins. Two of the main components of the intracellular cytoskeletal membrane are actin and spectrin. Bound to this network are various cellular proteins, one of which is ankyrin, that are also bound to transmembrane proteins. L1 interacts with the cytoskeleton both via an ankyrin binding site on the cytoplasmic domain and with actin via an unknown linker (Davis and Bennett, 1994; Dahlin-Huppe et al., 1997). The cytoplasmic domain of L1 contains multiple phosphorylation sites that could allow dynamic regulation of cytoskeletal interactions (Garver et al., 1997; Zisch et al., 1997; Heiland et al., 1998). Ankyrin mutant mice exhibit similar axonal misrouting, fasciculation and other axonal targeting defects to those shown in L1 mutant mice, suggesting that these two molecules may affect a common pathway in vivo (Scotland et al., 1998). L1 is recycled from the trailing to the leading edge of migrating

growth cones (Kamiguchi and Lemmon, 2000). Depending on the strength of the extracellular binding of cell adhesion molecules like L1, the shape and movement of the growth cone changes (for a review, see Suter and Forscher, 2000). If the recycling of L1 and its binding to ankyrin intracellularly (and therefore the cytoskeleton) are critical to growth cone movement and guidance, then we should see major defects in axon pathfinding and guidance in L1 mutants. Additionally, if ankyrin is a specific binding partner for L1, we might expect to see changes in ankyrin expression following chronic loss of L1.

We used the establishment of connections between the thalamus and cortex as our model because this is a system where axons make precise topographic, reciprocal connections and because L1 is present on thalamocortical and corticothalamic axons in the radiations and in the intermediate zone directly beneath the cortical target tissue of thalamic axons (Fushiki and Schachner, 1986; Chung *et al.*, 1991; Fukuda *et al.*, 1997). As early as day 10 of mouse embryonic development, axons in the marginal zone of the cortex express L1. By day 12 of development, within a half day of the earliest thalamic or cortical axon development, axons in the intermediate zone begin to express L1 (Fushiki and Schachner, 1986). These are presumably cortical axons since thalamic axons are not present at the subplate/cortex before embryonic day 14 (Molnar *et al.*, 1998; Del Rio *et al.*, 2000). These findings suggest that L1 is expressed on thalamocortical/corticothalamic axons during their initial formation and throughout the pathfinding process. To test the hypothesis that disruption of L1 alters normal thalamic axon pathfinding, including thalamocortical/corticothalamic fasciculation and/or target acquisition, we quantitatively examined the development of axonal connections between the thalamus and cortex in normal mice and mutant mice lacking L1.

Materials and Methods

Animals
All procedures described were carried out using protocols approved by the Vanderbilt Institutional Animal Care and Use Committee and the Freie und Hansestadt Hamburg. We used mice on a C57BL/6 background in which the L1 gene was mutated by insertion of thymidine kinase and neomycin resistance genes into exon number 9 of the L1 gene (Dahme *et al.*, 1997). We defined the day of conception [embryonic day 0 (E0)] as the day (morning) when a vaginal plug was detected after placing the male in the cage the night before. We always removed the male on that morning. We defined the day of birth as postnatal day zero or P0. We only made comparisons between age-matched mice (typically siblings).

General Preparation of Brains
Mice of known age were deeply anesthetized and a small sample of the tail or an ear punch was taken for genotyping. Experimental subjects were given a lethal dose of barbiturate and perfused transcardially with a saline rinse containing 0.4% sodium nitrate and then a fixative containing 4% paraformaldehyde and 0.1% glutaraldehyde or the same fixative with the addition of 0.1% EDTA (Hofmann and Bleckmann, 1999). Brains used for lipophilic labeling studies were dissected, inoculated with the dye(s) and then stored in the dark at room temperature in PBS or fixative containing 0.1% EDTA. After 6 weeks, the brains were moved to 4°C and stored until they were sectioned on a Vibraslice. Brains used for histochemistry or immunocytochemistry were perfused as described previously then removed to fixative containing 30% sucrose overnight at 4°C. Once the brains had equilibrated in the sucrose solution, they were stored at –70°C until they were sectioned frozen.

Lipophilic Dye Inoculations in the Cortex and Thalamus and Confocal Analysis
Following perfusion as described above, the two hemispheres of post-natal day zero (P0 or birth) or 2-week-old (P14) mice were separated and the midbrain was dissected away at the level of the habenula. We inserted small crystals of DiI, DiA and/or DiD into the dorsal thalamus. We made inoculations of lipophilic dye in 7 L1 mutant (five animals), 10 heterozygous (six animals) and 28 normal sibling (14 animals) thalami at P0. At P14, we inoculated one thalamus and the opposite side cortex of three mutant and three normal sibling animals. To examine thalamic axon invasion into cortex, we compared a mutant or heterozygous brain and a normal sibling brain with matching DiI inoculations in the thalamus. We examined seven L1 mutant, seven heterozygous and eight normal sibling hemispheres at P0. At P14, we examined both hemispheres of each animal. To examine thalamo-cortical projections, we placed DiD in the visual cortex and DiI and/or DiO in the somatosensory and/or motor cortex.

Vibratome sections (75–100 μm) were evaluated and photographed using a microscope equipped with an epifluorescent light source. For cases involving thalamic inoculations at both P0 and P14, we noted the depth of invasion of the thalamocortical axons and their regional distribution in cortex (topography). In addition, we examined and photographed individual branching axons and growth cones in the P0 animals. For all cases involving cortical inoculations, we examined the distribution of axons marked with different labels (with differently colored fluorescent tags) within the internal capsule and also within the thalamus. For unknown reasons, retrograde transfer of the lipophilic dyes was not as efficient as anterograde transfer at P14 despite inoculations that clearly encompassed thalamocortical target layers IV and VI. This could be a result of the increased level of myelination at this age, although it is unclear why myelination would affect diffusion of the label in only one direction.

Axon morphology in P0 mouse cortex was further analyzed under a Leica confocal laser scanning microscope. We collected multiple serial and montaged confocal images from five L1 mutant hemispheres (three animals), four heterozygous hemispheres (two animals), and six normal sibling hemispheres (six animals). Some sections were photoconverted with diaminobenzidine and counterstained so the borders of layers and nuclei could be detected (Singleton and Casagrande, 1996). To assess the growth cone morphology of the mutants directly, we imaged individual thalamic growth cones recording their laminar location in the cortex. We took confocal images of growth cones in an L1 mutant animal and a normal sibling with equivalent thalamic inoculations of DiI at P0. We measured well isolated, completely labeled growth cones in cortical layer V (L1+/+, n = 51; L1–/y, n = 25), VI (L1+/+, n = 29; L1–/y, n = 31) and the subplate (L1+/+, n = 10; L1–/y, n = 13). To measure each growth cone's two-dimensional length, we noted the distance between the neck, or thinnest portion of the axon adjacent to the growth cone and the tip of the longest filopodia in microns. Confocal images of growth cones were enlarged to show their morphology using a mathematical algorithm (Fig. 2; Genuine Fractals Print Pro, LizardTech Inc., Seattle, WA). In addition, an edge mask filter was used to enhance the resolution of the edges of the growth cones.

Quantification of Radiation Fascicle Size and Incidence of Pathfinding Errors
At P0 we examined eight hemispheres from seven L1 mutants, four hemispheres from two L1 heterozygotes and five hemispheres from five normal siblings for pathfinding errors in the radiations. We noted the extent and specific direction of any misrouting events. In one of the L1 mutant hemispheres, the DiI did not transport properly due to brain damage during removal from the skull; therefore, we excluded this hemisphere from all analyses. To quantify the size of fascicles in the radiations of the P0 mice, we examined five hemispheres from five animals wild-type for L1, four hemispheres from two L1 heterozygotes and four hemispheres from two homozygous L1 mutants. We also quantified the fascicles in three hemispheres of P14 L1 mutants and three normal sibling hemispheres. For each hemisphere examined, we chose one lateral saggital section in which the radiations were in cross-section for analysis. In mice there are only one or two sections in which the radiations appear in cross-section ensuring that measure-

ments were matched between cases. We imaged all labeled bundles in that section with the confocal microscope and imported each scanned image into an image analysis system, Bioquant (Nashville, TN) for P0 brains or Zeiss LSM510 software for P14 brains. Each bundle was outlined by hand after thresholding and the area was calculated using the respective software. We did not include single axons or bundles of three or fewer axons in the analysis.

Documentation of Cortical Lamination and Thickness
To examine the formation of cell layers in the cortex, we stained some sections for Nissl substance. Sections were mounted out of buffer, dried, dehydrated through an ascending series of alcohols and then stained with a solution containing 1% cresyl violet. We used Nissl-stained sections of P0 and 4-week-old mice to measure the thickness of the cortex in normal animals and L1 mutants. Because we did not stain sections of P14 brain for Nissl substance, measurements in these animals were made on vibratome sections viewed under darkfield. Note that measurements could not be compared across ages given differential shrinkage of tissue that occurs in hydrated (vibratome) versus dehydrated (Nissl-stained) tissue. To quantify cortical thickness two measurements were taken from cortex dorsal to the anterior and posterior margins of the granule cell layer of the hippocampus and perpendicular to the cortical surface. To quantify cortical thickness in P0 L1 mutants, we measured two hemispheres from one normal animal, two hemispheres from two heterozygous animals and two hemispheres from two mutant animals. At P14, we measured three hemispheres from three normal animals and three hemispheres from three mutant siblings. At 4 weeks, we measured one hemisphere from one normal animal and two hemispheres from two L1 mutants.

Statistical Analysis
Statistical analysis was performed using Sigmastat 3.0 software and graphs were produced with the aid of Sigmaplot 8.0 software (SPSS Inc., Chicago, IL). In cases where two groups were compared, a Student's t-test was used when data were normal and had equal variance. Otherwise, a nonparametric test was used, the Mann–Whitney rank sums test. In cases where three or more groups were compared and the data were skewed, a Kruskal–Wallis one-way ANOVA on ranks was used. In the latter cases, post-hoc analyses with Dunn's all pairwise multiple comparison procedures were used to decide which genotypes were significantly different. We accepted a 95% confidence level as significant.

Immunocytochemical Protocol
For immunocytochemistry, we sectioned hemispheres in the saggital plane on a freezing microtome at 20 µm into Tris-buffered saline (TBS) and placed these sections into a solution of TBS containing 60% methanol for 20–30 min at room temperature. After three rinses in TBS, sections were incubated for 20 min at room temperature in a 0.1 M glycine solution, pH adjusted to 7.4 with 1 M Tris base. Immunolocalization of ankyrin-B was enhanced when sections were steamed for 20 min in citrate buffer, pH 6.0, before the blocking buffer step. Two more rinses in TBS were followed by a 2 h incubation in blocking buffer containing 10% normal donkey serum, 0.2 M lysine, 0.2 M glycine and 0.1% Triton-X 100 in TBS. Without rinsing, the sections were placed into antibody solution with 3% normal donkey serum, 0.2% cold water fish gelatin, 0.1% Triton-X 100 and 1:250 α-ankyrin-B (Research Diagnostics Inc., RDI-ANKYRBabmX) at 4°C for 48 h with agitation. The ankyrin-B antibody is directed against the portion of the ankyrin-B protein that binds to spectrin. After three rinses with TBS plus 2% cold water fish gelatin, sections were placed into the same antibody buffer with donkey α-mouse biotinylated secondary antibody (Chemicon, AP192B) for 2 h at room temperature. After three more washes, sections were placed into the rinse buffer with 1:500 streptavidin-Cy3 (016-160-084; Jackson Labs) in the dark for 2 h at room temperature. We then mounted sections on gelatinized slides, coverslipped them with vectashield (PK-6100; Vector Labs) and stored them in the dark at 4°C until we could analyze them.

Results

Axon/Growth Cone Morphology and Targeting in Cortex
We examined several aspects of thalamocortical axon innervation in each mutant, including: the degree of fasciculation of axons in the radiations, initial invasion of the intermediate zone of the cortex, branching into the subplate from the intermediate zone (i.e. formation of a simple initial T-shaped branch), growth and/or invasion of axons into the base of the cortical plate (developing layers V and VI), branching of axons within the cortical plate, depth of invasion of thalamic axons into the cortical plate, the morphology of growth cones during all these processes and, finally, correct target acquisition. Qualitative examination of the thalamocortical pathway in P0 mutant mice revealed that axons in the radiations are hyperfasciculated and some thalamocortical axons are misrouted (see Fig. 1). In these L1 mutants, the radiations consist mainly of a few large fascicles of axons coursing through the basal ganglia. The most posteriorly located axon fascicles are the most affected by the mutation and, in all newborn cases examined, the most posterior fascicle(s) was observed to make a sharp posterior turn toward the lateral ventricle. This specific pathfinding error occurred in 100% of the L1 mutants examined and in none of the normal or heterozygous sibling animals at P0. Closer examination revealed that when the misrouted axons reach the lateral ventricle, fasciculation is lost. It does not
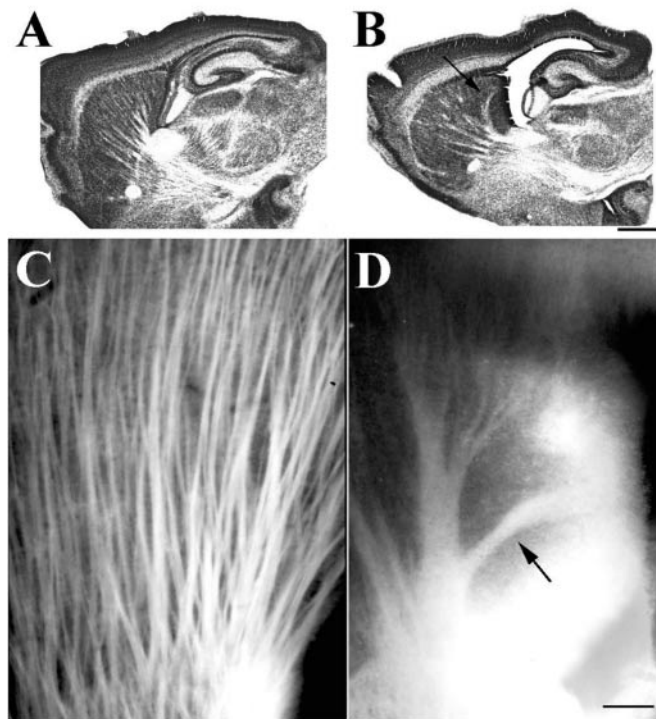
Figure 1. Misrouting of thalamocortical axons in newborn L1 mutants. Photomicrographs of Nissl-stained sections (A, B) and DiI labeled axon fascicles (C, D) within the radiations. In these saggital sections, dorsal is toward the top and anterior is to the left. Note the large size of the bundles in L1 mutants (B, D) compared with normal siblings (A, C). One large bundle of axons (see arrow) exhibits clear misrouting and heads for the ventricular wall (toward the right) instead of the cortex (D). This axon pathfinding error is apparent even with the cell stain only in another animal (see arrow, B). When the bundle gets close to the wall, fasciculation is lost (D). Scale bar is 50 µm in A and B, 100 µm in C and D.

appear that these axons continue toward the cortical plate at this stage of development. By 2 weeks of age, there is no more evidence of misrouting although the defect in fasciculation remains robust and can easily be seen at 4 weeks as well. It seems likely that the misrouted axons or cells that provide these axons are culled during the period of cell death and axon remodeling that follows the initial invasion of axons into the cortex.

Growth cone morphology also showed subtle abnormalities in L1 mutants. The L1 mutant growth cone processes were qualitatively more complex and quantitatively longer (see Fig. 2). To quantitatively test the hypothesis that the L1 mutation affects the morphology of growth cones, we measured the length of growth cones in identified cortical layers at birth. In the subplate, L1 mutant growth cones (8.2 ± 0.7 μm; mean ± SEM) were longer than normal growth cones (5.9 ± 0.5 μm; t-test, $P = 0.026$). In layer VI, we found no significant difference between L1 mutant (8.3 ± 0.5 μm) and normal growth cones (7.7 ± 0.5 μm; t-test, $P = 0.477$). In layer V, we found no significant difference between L1 mutant (10.5 ± 1.0 μm) and normal growth cones (9.8 ± 0.5 μm; rank sum test, $P = 0.956$). The subplate separates the intermediate zone, where axons travel, from the cortical plate proper and can be considered an important choice point for axons selecting appropriate cortical targets. Loss of L1 changes growth cone morphology significantly only in the subplate.

Quantification of Fasciculation in the Radiations

As expected from our initial qualitative observations, L1 mutants have significantly larger fascicles within the thalamo-cortical radiations than normal animals at all three ages studied (see Fig. 3A). Fascicle size in L1 mutants (2480 ± 374 μm²;

mean ± SEM) was significantly different from that in L1 hetero-zygotes (354 ± 21 μm²) and normal siblings (346 ± 27 μm²; ANOVA, $P \leq 0.001$) at birth. Post-hoc analysis revealed that only L1 mutants, not L1 heterozygous animals, have hyperfas-ciculated fascicles at P0 (Dunn's multiple comparison, $P < 0.05$). At 2 weeks of age, fascicles are still significantly larger in L1 mutants (1474 ± 261 μm²) than in normal animals (379 ± 25 μm²; rank sum test $P \leq 0.001$). Although slightly different methods were used to collect the fascicle diameter data, the distribution of normal fascicle sizes at 2 weeks was remarkably like that at P0 (see Fig. 3B). The latter observation assures us that the methods used to collect the data were robust.

Cortical Lamination and Organization of Cortical Afferents

To ascertain whether mutant mice produce all layers normally, we examined cortical lamination in Nissl stained sections. At P0 in normal animals, layers V and VI have migrated to their respective positions in the cortical plate (Caviness, 1982; Del Rio *et al.*, 2000). At 4 weeks of age, normal mice have all
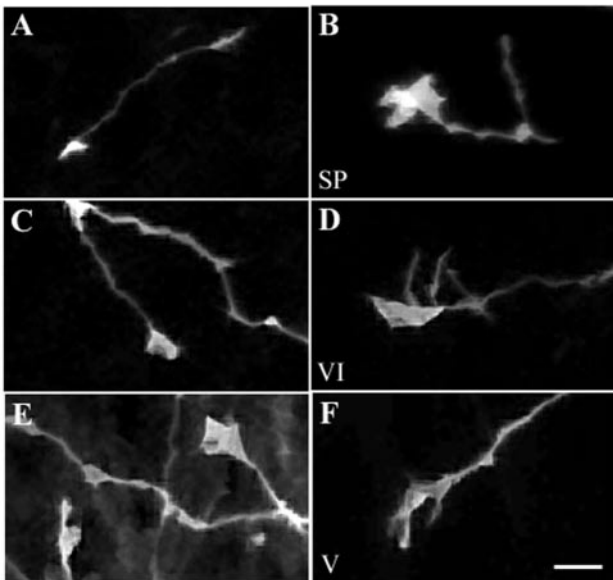
Figure 2. Growth cone morphology of thalamic axons in the cortex of L1 mutants. We examined the invasion of thalamic axons into the cortex in normal mice (*A*, *C*, *E*) and L1 mutant mice (*B*, *D*, *F*). Growth cones in the subplate (SP; *A*, *B*), cortical layer VI (*C*, *D*) and layer V (*E*, *F*) were examined and measured. As expected in normal animals, growth cones become larger and more complex as they ascend into the cortex. L1 mutants had qualitatively more complex growth cones with numerous long filopodia. Quantitatively, growth cones were longer in the subplate in L1 mutants. See text for details. Scale bar is 10 μm.
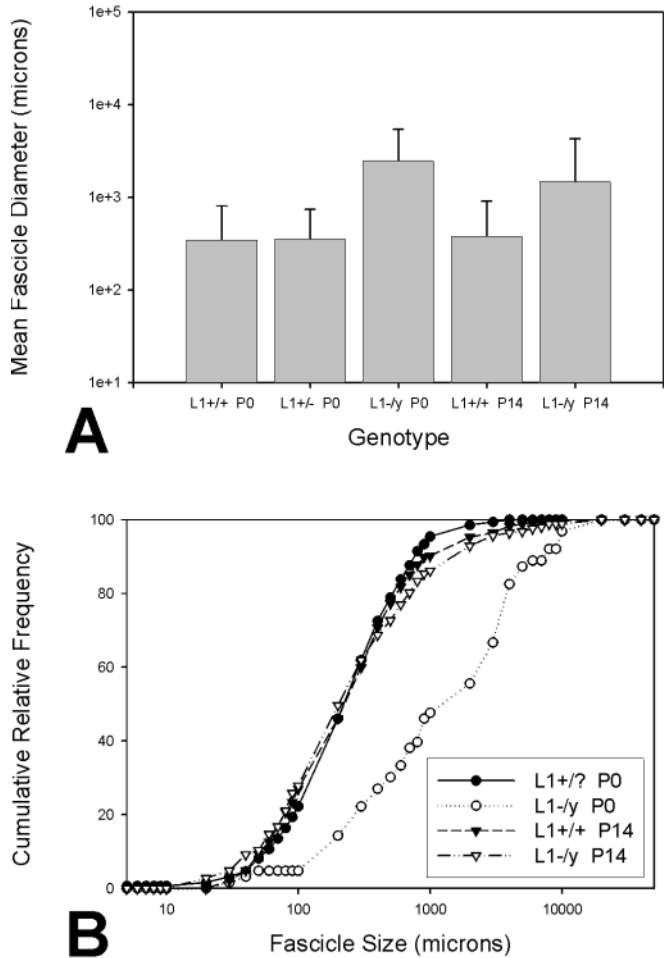
Figure 3. Quantitative differences in fascicle size in L1 mice. (*A*) At birth, fascicles in L1 mutants (L1–/y) were significantly larger than in normal or heterozygous animals (ANOVA, $P \leq 0.001$). At 2 weeks of age, fascicles in L1 mutants were still significantly larger than those in normal siblings (rank sum test, $P \leq 0.001$). Error bars represent standard error of the mean. (*B*) When the data are arranged by cumulative relative frequency, it is clear that the P14 L1 mutants exhibit less of a hyperfasciculation defect compared to P0 mutants. See text for details.

cortical layers and an essentially adult phenotype. All cortical layers normally present are present in L1 mutant mice at P0, 2 weeks and 4 weeks of age. Clearly L1 is not a prerequisite for the final migration of cells to form cortical layers since most regions of the cortex develop appropriately in its absence. To quantitatively compare cortical thickness in mutant and normal mice, we measured the thickness of the cortical plate at P0, 2 weeks and at 4 weeks of age. L1 mutants have a significantly thinner cortex at P0 with heterozygotes intermediate, but by 2 weeks of age the cortex of the L1 mutant is not significantly thinner (see Fig. 4). At P0, the average thickness of the cortical plate of L1 mutants is 254 ± 8 μm (mean $\pm$ SEM), that of L1 heterozygotes is 329 ± 6 μm and that of normal siblings is 403 ± 13 μm. Statistical comparison reveals that these are significantly different (ANOVA, $P \leq 0.001$). This transient difference in cortical thickness could reflect a delay in the normal migration process of some neurons. At 2 and 4 weeks of age, the cortex of L1 mutants (1084 ± 19 μm and 513 ± 7 μm, respectively) is no longer significantly different from that of normal siblings (1052 ± 18 μm, rank sum test, $P = 0.310$ at P14 and 518 ± 16 μm, rank sum test, $P = 0.990$ at P28).

One aspect of thalamocortical innervation that is important to address is the fidelity of areal and topographic axonal connections in the mutants. To address the issue of areal specificity in L1 mutants, we inoculated different cortical regions with a series of of lipophilic dyes that fluoresced different colors. Results of these different dye inoculations always indicated that visual cortex was innervated by visual thalamic nuclei, motor cortex by motor thalamic nuclei and somatosensory cortex by somatosensory thalamic nuclei (see Fig. 5A,B). To address the issue of topographic specificity we looked at several indicators. Multiple inoculations of different colors of lipophilic dyes in the thalamus (see Fig. 5C,D) or cortex (see Fig. 5E) resulted in multicolor labeling of fascicles in the radiations. Any given fascicle tended to be a single color suggesting that topographic specificity is maintained to some extent in the internal capsule. Additionally, single small inocu-

lations in the visual thalamus at 2 weeks of age resulted in precise patches of label in the cortex, with clouds of anterogradely labeled axons in layer IV located directly above patches of retrogradely labeled cells in layer VI (data not shown).

In addition, we examined the barrel field in somatosensory cortex. In mice each facial vibrissa provides input to a special cluster of cortical cells called a barrel (because of its appearance in a Nissl stain) in the somatosensory cortex (Woolsey and Van der Loos, 1970; Jensen and Killackey, 1987). These barrels or modules in cortical layer IV form an exact map of all of the facial vibrissae on each side of the face, a map that occupies a large proportion of mouse cortex. Thalamocortical axons enter somatosensory cortex in an organized fashion such that bundles of fibers carrying information about an individual whisker enter the cortex together; however, the cells in cortex do not begin to organize into barrels until after birth (Killackey *et al.*, 1995). We examined this aspect of somatosensory development in L1 mutant mice at 2 and 4 weeks of age. L1 mutants have normal barrels as defined by cell staining (see Fig. 6). This finding suggests that thalamocortical target acquisition, in somatosensory cortex at least, occurs normally in animals missing the cell adhesion molecule L1.

Ankyrin-B Expression in L1 Mutant Mice
One of our goals was to investigate the link between L1 and the cytoskeleton. In an initial attempt to probe the link between L1 and ankyrin-B, we tested for the presence of ankyrin-B in L1 mutants. At P0 ankyrin-B is mainly expressed on unmyelinated axons spread throughout the cortical plate, the ganglionic eminence and the thalamus, an expression pattern mirroring that of L1 (Chan *et al.*, 1993). Surprisingly, although spectrin expression is unchanged (data not shown), the expression of ankyrin-B is lost throughout the brain in L1 mutant mice (see Fig. 7). This finding suggests that L1 may be involved in the regulation of Ank2, the gene that encodes for ankyrin-B, or the maintenance of its stability.

Discussion
Our main findings are that thalamocortical and corticothalamic axons in mice lacking L1 are hyperfasciculated, a subset of thalamocortical axons makes a consistent and specific pathfinding error in the internal capsule at P0, and thalamocortical axon growth cones are more complex and longer than normal in the subplate. These defects occur despite normal formation of six cortical layers and formation of areally and topographically appropriate thalamocortical connections. The loss of L1 is accompanied by loss of expression of ankyrin-B, an intracellular L1 binding partner, suggesting that L1 is involved in the regulation of Ank2 stability and underscoring the close relationship between cell adhesion molecules and cytoskeletal elements. We postulate that the pathfinding errors, growth cone abnormalities and hyperfasciculation of axons following loss of L1 reflect both a shift in binding partners among axons and different substrates and a loss of appropriate interactions with the cytoskeleton. This perspective is defended in light of recent research in the discussion below.

At birth, thalamocortical growth cones appear normal in L1 mutants in all cortical layers except the subplate, where the mutant growth cones are significantly longer and subtly more complex than normal. The structure of the growth cone affects the subsequent structure of the axon and is linked to the
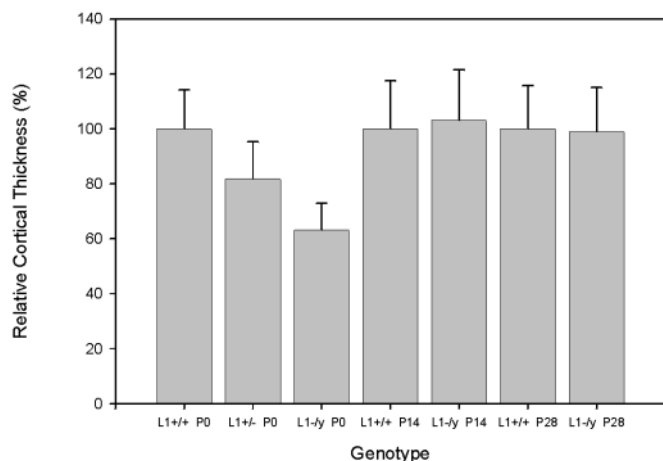

Figure 4. Thickness of the cortical plate in L1 mutants from birth (P0) to 4 weeks of age. L1 mutants have significantly thinner cortical plates at P0 than normal animals, while L1 heterozygotes have a cortical plate of intermediate thickness. L1 mutants at 2 and 4 weeks of age do not differ from wild type siblings in cortical thickness. Error bars show standard error of the mean.
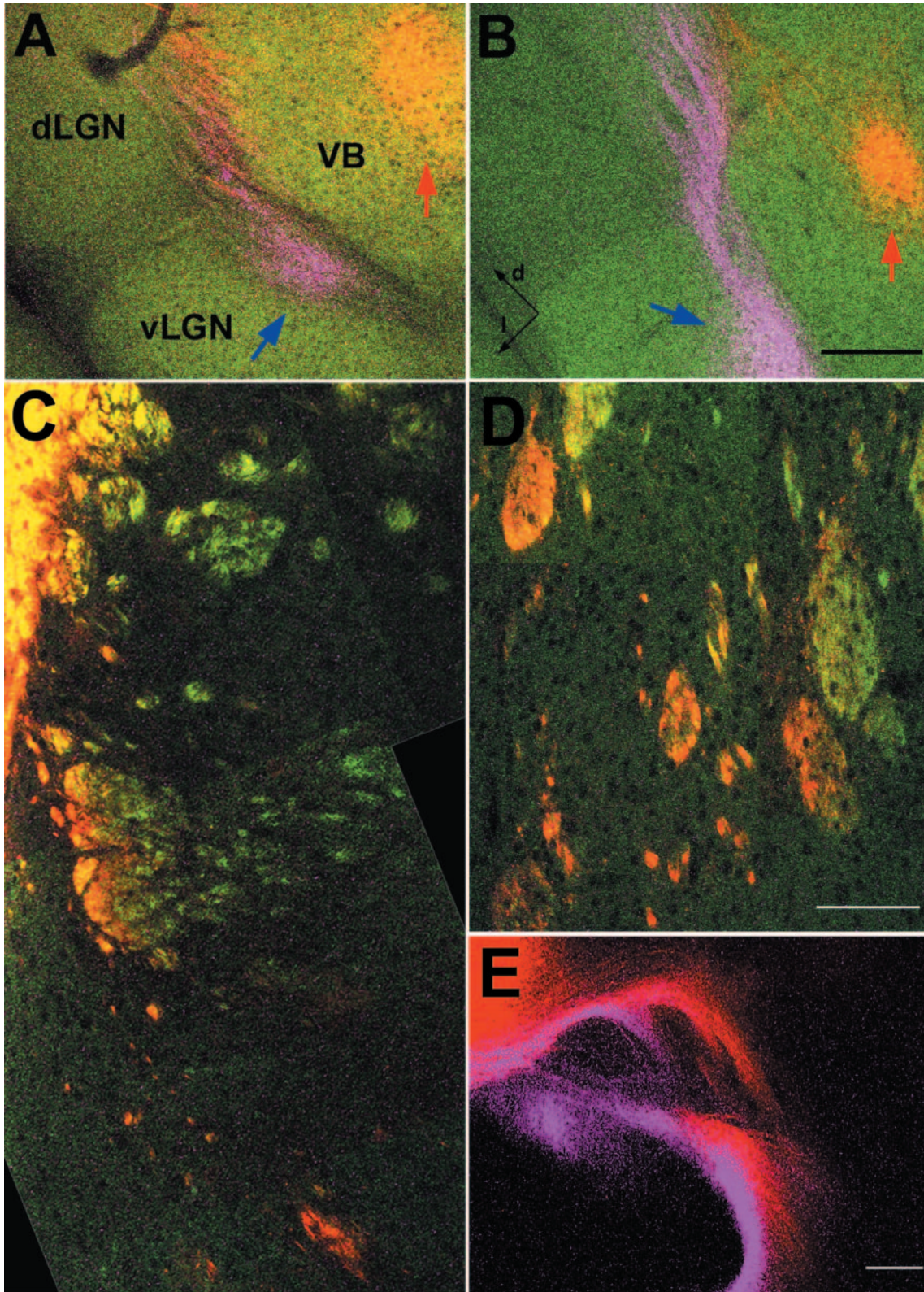
Figure 5. L1 mutants show areal and topographic specificity at 2 weeks of age. (*A, B*) Anterograde transport of lipophilic dyes from cortex to the dorsolateral thalamus is shown for a normal animal (*A*) and a mutant sibling (*B*). The images are tilted to the left, dorsal (d) is toward the top and left and lateral (l) is toward the bottom and left. Dil (red arrow) was placed in the somatosensory cortex and transported to the ventrobasal nucleus of the thalamus (VB). DiD (blue arrow) was placed in the visual cortex and transported to the ventral lateral geniculate nucleus (vLGN). The dorsal lateral geniculate nucleus (dLGN) is indicated for orientation. (*C, D*) Examples of fascicles labeled by inoculations of Dil (red) and DiO (green) in the thalamus that were measured in a normal mouse (*C*) and an L1 mutant sibling (*D*) are shown by photomontage. Note that there are fascicles that are labeled with each color preferentially indicating that at least rough topography is maintained in the internal capsule in L1 mutants. The anterior margin of the lateral ventricle is towards the left of each image and dorsal is toward the top. (*E*) An example of double labeled corticothalamic axons entering the internal capsule after Dil (red) and DiD (purple) were placed in different regions of the cortex of an L1 mutant. Note the segregation of the two colors. Scale bar is 200 μm in *A, B* and *E* and 100 μm in *C* and *D*.
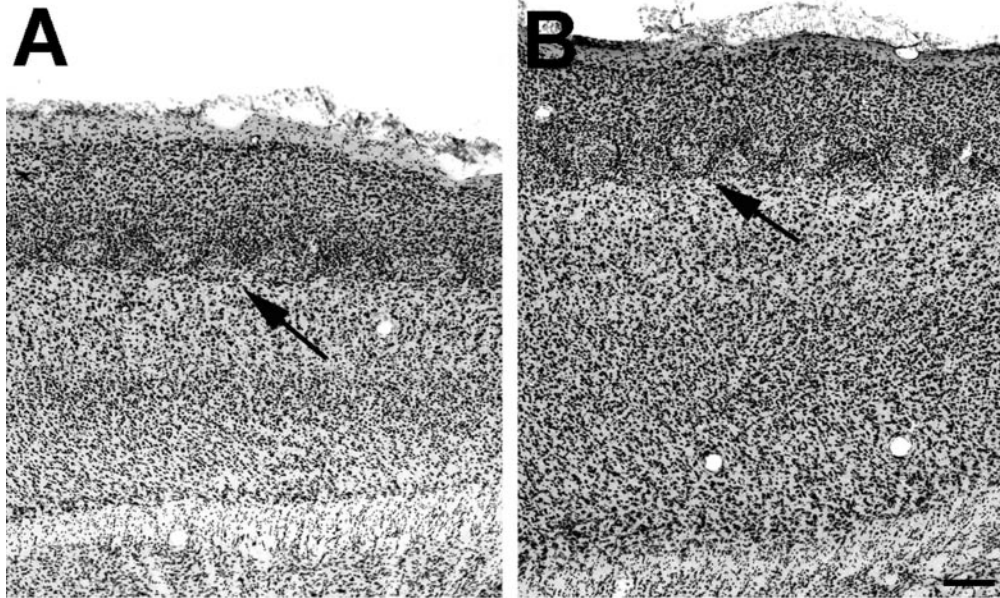
Figure 6. L1 mutants have barrels in the somatosensory cortex at 4 weeks of age. Photomicrographs of Nissl-stained sections through the barrel field in layer IV of somatosensory cortex at 4 weeks postnatal in a normal mouse (*A*) and an L1 mutant (*B*). Dorsal is toward the top. Note the well developed barrels in cortical layer IV in both mutant and wild-type animals (arrows). Note also that sections are not from identical regions of the barrel field. Cortical thickness was in the normal range in L1 mutants at 4 weeks (see Fig. 4). Scale bar is 100 μm.
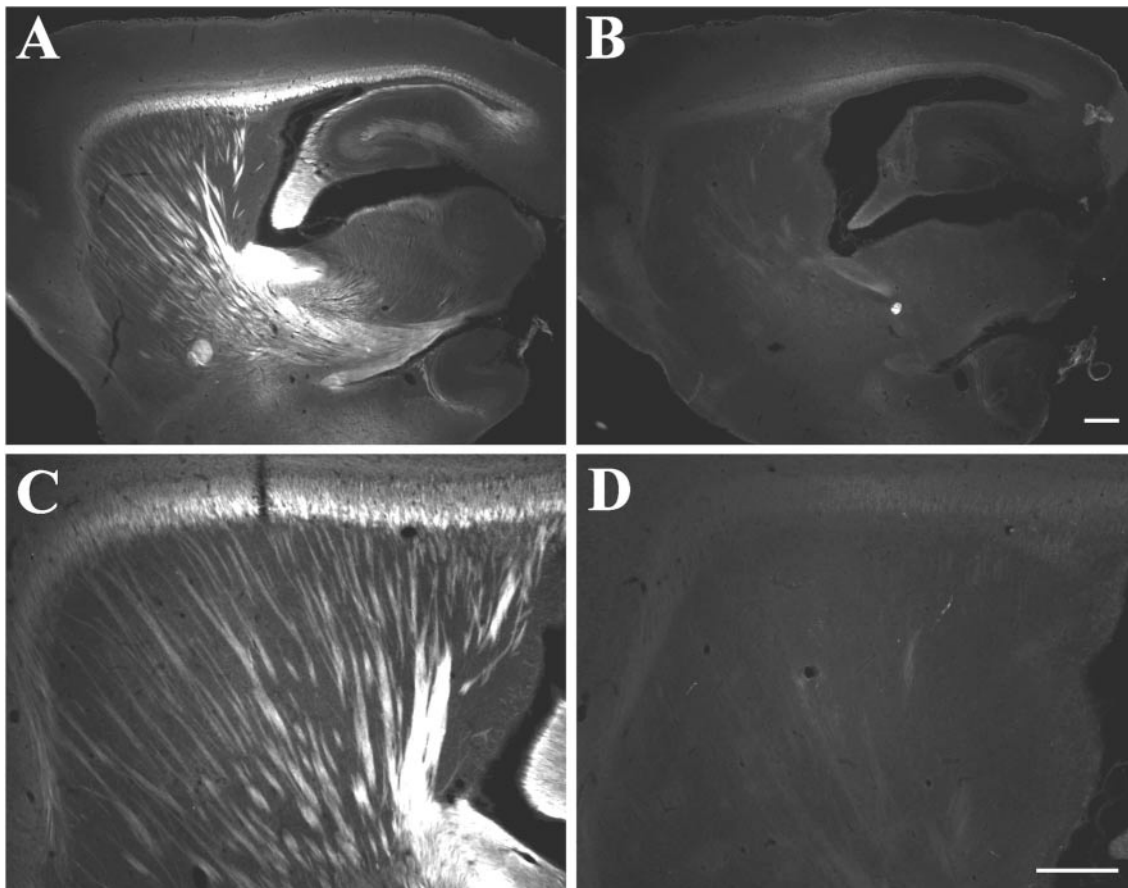

Figure 7. Decreased ankyrin-B expression in L1 mutants. Immunocytochemistry for ankyrin-B revealed that its expression in normal animals (*A, C*) is lost in L1 mutants (*B, D*). Note that ankyrin-B is expressed in an identical pattern to L1 at P0, mainly on axons. In these saggital sections, dorsal is towards the top and posterior is to the right. Scale bar is 200 μm.

steering behavior of the growth cone (Mason and Wang, 1997; Szebenyi *et al.*, 1998; Davenport *et al.*, 1999). Additionally, modifications of the cytoskeleton are intimately associated with changes in the shape of the growth cone (Lin *et al.*, 1994; Dent *et al.*, 1999; for a review see Letourneau, 1996). The fact that growth cones without L1 are longer in the subplate suggests that the loss of L1 disrupts the cell adhesion machinery of the migrating growth cone as suggested by the 'substrate-cytoskeletal coupling' model (Mitchison and Kirschner, 1988; Lin *et al.*, 1994; Suter *et al.*, 1998; Suter and Forscher, 2000). If this model were correct, however, the expectation would be that loss of L1 would result in total loss of forward movement by axons. Additionally, if L1 is simply an adhesive element in the growth cone, then it is unclear why we see evidence of increased adhesiveness in the radiations between axons that normally express L1 in L1 mutants. Despite *in vitro* findings that homophilic L1 binding promotes growth of axons (Lagenaur and Lemmon, 1987; Lemmon *et al.*, 1989; Fransen *et al.*, 1998), the most reasonable explanation for our results is that L1 normally functions in the thalamocortical radiations by binding heterophilically to the substrate.

Another aspect of the 'substrate-cytoskeletal coupling' model of growth cone advance is the connection of L1 with ankyrin inside the cell (Long and Lemmon, 2000). This link and the binding of ankyrin to the cytoskeleton provide the anchor against which the growth cone is thought to pull in order to move forward or change directions (Davis and Bennett, 1994). In our experiments, we found that ankyrin-B expression is lost in L1 mutant mice. The hyperfasciculation and misrouting that we see in L1 mutants at birth is associated with the loss of both L1 and ankyrin-B. This suggests that ankyrin-B, normally coexpressed with L1 on thalamocortical/corticothalamic axons (see Fig. 7; Chan *et al.*, 1993), is a specific binding partner for L1 and that L1 might be involved in the production and/or stabilization of Ank2 (Bennett and Lambert, 1999). In fact, studies have shown that *Drosophila* mutants missing neuroglian (a homologue of L1) have decreased expression of Dank2 (a second, novel homologue of mammalian ankyrin) suggesting that neuroglian stabilizes Dank2 (Bouley *et al.*, 2000). The simplest explanation is that L1 and ankyrin-B are normally involved in defasciculation in the radiations and that they work in concert. Without L1, presumably growth cones advance using another mechanism that does not involve ankyrin-B but could involve other L1 and ankyrin family members.

Alternatively, L1 may participate in contact-mediated repulsion via interactions with semaphorins (see Fig. 8; Castellani, 2002). Sema-1a on *Drosophila* motor axons acts to induce defasciculation at specific choice points by countering the attractive force of fasII, an invertebrate homologue of NCAM, and conn (connectin; Yu *et al.*, 2000). Cortical axons lacking L1 fail to respond to Sema3a, a repulsive ventral spinal cord signal. Addition of L1Fc chimeric molecules to the co-cultures changed the Sema3a-induced repulsion of wild-type cortical axons into an attraction but did not affect L1-deficient axons (Castellani *et al.*, 2000). These findings suggest that L1 and Sema3a are in the same pathway and that L1 mutants may have guidance errors directly caused by the failure of Sema3a signals (Castellani *et al.*, 2002). Additionally, cortical layer V cells project across the callosum as well as to the tectum and spinal cord. Perhaps these pathways are disrupted in the L1 mutants
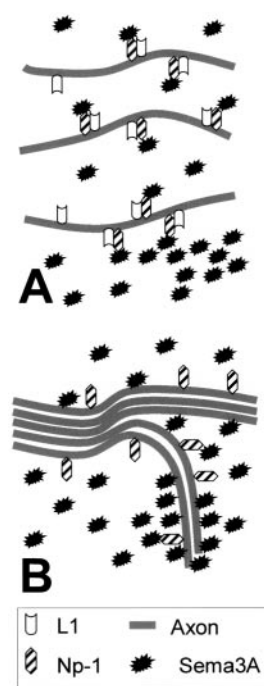
Figure 8. The role of L1 in fasciculation: interactions with neuropilin and semaphorin. One hypothesis for the hyperfasciculation and pathfinding defects we see in L1 mutant animals is that L1 normally binds to neuropilin-1 on thalamocortical/corticothalamic axons and this complex is a receptor for the repulsive molecule semaphorin 3A located in the radiations. Signaling through this complex normally results in normal fasciculation levels and avoidance of the ventricular wall by axons (*A*). Instead, in L1 mutants, thalamocortical/corticothalamic axons fail to defasciculate and make a wrong turn toward the ventricle (downwards in the schematic; *B*). With the caveat that other molecules are probably involved, this hypothesis could be tested as follows: (i) loss of neuropilin in thalamic cells should produce the same phenotype as loss of L1; (ii) a L1–/y, semaphorin 3A –/– double mutant mouse should show no defects in fasciculation.

because of interactions between Sema3a and L1. In support of this hypothesis, Sema3a is expressed in the internal capsule while axons are making connections between the thalamus and cortex (Skaliora *et al.*, 1998).

It has been suggested that Sema3a is involved in maintaining segregated thalamic and cortical axon fiber tracts in the intermediate zone/subplate (Bagnard *et al.*, 2001). In fact, in the peripheral nervous system of the chick, application of functionally blocking L1 antibodies caused sensory axons to fail to segregate into the appropriate nerves (Honig *et al.*, 2002). Perhaps the hyperfasciculation defect we describe here results from a failure of thalamic and cortical axons to segregate in the internal capsule. We did not directly test this hypothesis. Interestingly, the noted misrouting in the chick was accompanied by changes in the caliber or shape of individual axons in cross-section suggesting that L1 is important during the packing of axons into bundles and that loss of such an adhesive property leads to errors in pathfinding (Honig *et al.*, 2002).

It seems that one consistent property of axons that have lost L1 is that they sometimes ignore guidance cues, probably negative cues but not necessarily. For example, murine axons lacking L1 fail to stop in the anterior tectum and some fail to stop in the tectum at all (Demyanenko and Maness, 2003). In our experiments, loss of L1 results in the production of larger growth cones in the subplate but not the rest of the cortical plate in newborn animals. Here, L1 must normally either instruct growth cones to adhere less to the substrate or it must

mediate a repulsive cue. It seems unlikely that a secreted signal, such as Sema3a, could be responsible for a layer-specific effect on a growth cone unless it was produced at low levels in a very discreet, laminar pattern. An alternative would be interactions between L1 and the transmembrane semaphorins, which are actually more numerous (Raper, 2000). In fact, careful studies of retinal axons as they enter the optic disk have shown that antibodies which functionally block transmembrane Sema5a cause L1 positive axons to misroute and fail to enter the optic disk. They illustrate a misrouting event that looks remarkably like our Fig. 1 (see fig. 6*E* in Oster *et al.*, 2003). The authors hypothesize that Sema5a performs an ensheathing function, isolating the retinal pathway. When it is missing, the retinal axons are able to exit the pathway, whereas there are no exits when Sema5a is present.

Perhaps our misrouting event is caused by just such a loss of an ensheathing factor. Maybe one needs the adhesion molecule, L1, to be present in order to respond to certain cues in the substrate, cues such as semaphorins. This could be put into effect by a mechanism as simple as a shortening of the distance between neighboring membranes via L1 homophilic interactions as well as a number of more complicated schemes. Examination of L1 postive axons that have lost shared membrane regions following blocking of L1 function with antibodies supports such a simple theory (Honig *et al.*, 2002). When the ignored cues are negative or repulsive, then loss of L1 causes axons to misroute and form larger growth cones. When the ignored cues are positive, then the loss of L1 causes axons to hyperfasciculate rather than cling to the substrate. Since we can not discriminate between these two options, any given action by L1 may be a result of either a negative or positive interaction. In fact there is support in the literature for L1′s involvement in both adhesive and repulsive interactions depending on its structure and binding partners (Castellani *et al.*, 2002) and the same can be said for at least one of the semaphorins, Sema3A (Polleux *et al.*, 1998).

It is noteworthy, however, that the L1 mutant phenotype of hyperfasciculation that we see *in vivo* is in contrast to previous findings *in vitro*, although this change may be indicative of the cell type involved. L1 or L1 family members perform variable roles in axon fasciculation in several species (Fischer *et al.*, 1986; Rathjen *et al.*, 1987; Landmesser *et al.*, 1988; Bastmeyer *et al.*, 1995; Weiland *et al.*, 1997; Honig *et al.*, 1998; Hrynkow *et al.*, 1998; Kunz *et al.*, 1998; Xiao *et al.*, 1998). Fasciculation in major axon pathways is not always abnormal in the L1 mutant. For instance, the optic nerve forms a normal fascicle in L1 mutant mice, but then those axons go on to terminate inappropriately in the tectum (Demyanenko and Maness, 2003). Because of the promiscuous nature of cell adhesion, the combination of adhesive and repulsive elements in the substrate and on the axon may be extremely important to the behavior of individual types of axons during transit. The fasciculation phenotype seen in cells lacking L1 may be reliant on the particular adhesive nature of the substrate those cells contact and the particular time point in ontogenetic development. In other words, the specific subset of adhesive and repulsive elements present on the surface of axons and on the surfaces contacted by those axons may have different effects in different brain regions and/or developmental time points, an explanation that remains to be tested. Combine this potential diversity with the potential for a single molecule to provide cues of a positive or negative nature depending on its binding partners and one arrives at a complicated web of interactions that just might be able to specify the connectivity of a complicated brain.

References

Bagnard D, Chounlamountri N, Puschel AW, Bolz J (2001) Axonal surface molecules act in combination with semaphorin 3A during the establishment of corticothalamic projections. Cereb Cortex 11:278–285.

Bastmeyer M, Ott H, Leppert CA, Stuermer CA (1995) Fish E587 glycoprotein, a member of the L1 family of cell adhesion molecules, participates in axonal fasciculation and the age-related order of ganglion cell axons in the goldfish retina. J Cell Biol 130:969–976.

Bennett V, Lambert S (1999) Physiological roles of axonal ankyrins in survival of premyelinated axons and localization of voltage-gated sodium channels. J Neurocytol 28:303–318.

Bouley M, Tian MZ, Paisley K, Shen YC, Malhotra JD, Hortsch M (2000) The L1-type cell adhesion molecule neuroglian influences the stability for neural ankyrin in the *Drosophila* embryo but not its axonal localization. J Neurosci 20:4515–4523.

Brummendorf T, Kenwrick S, Rathjen FG (1998) Neural cell recognition molecule L1: from cell biology to human hereditary brain malformations. Curr Opin Neurobiol 8:87–97.

Castellani V (2002) The function of neuropilin/L1 complex. Adv Exp Med Biol 515:91–102.

Castellani V, Chedotal A, Schachner M, Faivre-Sarrailh C, Rougon G (2000) Analysis of the L1-deficient mouse phenotype reveals crosstalk between sema3a and L1 signaling pathways in axonal guidance. Neuron 27:237–249.

Castellani V, De Angelis E, Kenwrick S, Rougon C (2002) Cis and trans interactions of L1 with neuropilin-1 control axonal responses to semaphoring 3A. EMBO J 21:6348–6357.

Caviness VS Jr (1982) Neocortical histogenesis in normal and reeler mice: a developmental study based upon [³H]thymidine autoradiography. Brain Res 256:293–302.

Chan W, Kordeli E, Bennett V (1993) 440-kD AnkyrinB: structure of the major developmentally regulated domain and selective localization in unmyelinated axons. J Cell Biol 123:1463–1473.

Chung WW, Lagenaur CF, Yan Y, Lund JS (1991) Developmental expression of neural cell adhesion molecules in the mouse neocortex and olfactory bulb. J Comp Neurol 314:719–723.

Cohen NR, Taylor JHS, Scott LB, Guillery RW, Soriano P, Furley AJW (1997) Errors in corticospinal axon guidance in mice lacking the neural cell adhesion molecule L1. Curr Biol 8:26–33.

Crossin KL, Krushel LA (2000) Cellular signaling by neural cell adhesion molecules of the immunoglobulin superfamily. Dev Dyn 218:260–279.

Dahlin-Huppe K, Berglund EO, Ranscht B, Stallcup WB (1997) Mutational analysis of the L1 neuronal cell adhesion molecule identifies membrane-proximal amino acids of the cytoplasmic domain that are required for cytoskeletal anchorage. Mol Cell Neurosci 9:144–156.

Dahme M, Bartsch U, Martini R, Anliker B, Schachner M, Mantei N (1997) Disruption of the mouse L1 gene leads to malformations of the nervous system. Nat Genet 17:346–349.

Davenport RW, Thies E, Cohen ML (1999) Neuronal growth cone collapse triggers lateral extensions along trailing axons. Nat Neurosci 2:254–259.

Davis JQ, Bennett V (1994) Ankyrin binding activity shared by the neurofascin/L1/NrCAM family of nervous system cell adhesion molecules. J Biol Chem 269:27163–27166.

Del Rio JA, Martinez A, Auladell C, Soriano E (2000) Developmental history of the subplate and developing white matter in the murine neocortex. Neuronal organization and relationship with the main afferent systems at embryonic and perinatal stages. Cereb Cortex 10:784–801.

Demyanenko GP, Maness PF (2003) The L1 cell adhesion molecule is essential for topographic mapping of retinal axons. J Neurosci 23:530–538.

Demyanenko GP, Tsai AY, Maness PF (1999) Abnormalities in neuronal process extension, hippocampal development and the ventricular system of L1 knockout mice. J Neurosci 19:4907–4920.

Dent EW, Callaway JL, Szebenyi G, Baas PW, Kalil K (1999) Reorganization and movement of microtubules in axonal growth cones and developing interstitial branches. J Neurosci 19:8894–8908.

Fischer G, Kunemund V, Schachner M (1986) Neurite outgrowth patterns in cerebellar microexplant cultures are affected by antibodies to the cell surface glycoprotein L1. J Neurosci 6:605–612.

Fransen E, Van Camp G, Vits L, Willems PJ (1997) L1-associated diseases: clinical geneticists divide, molecular geneticists unite. Hum Mol Genet 6:1625–1632.

Fransen E, D'Hooge R, Van Camp G, Verhoye M, Sijbers J, Reyniers E, Soriano P, Kamiguchi H, Willemsen R, Koekkoek SKE, De Zeeuw CI, De Deyn PP, Van der Linden A, Lemmon V, Kooy RF, Williams PJ (1998) L1 knockout mice show dilated ventricles, vermis hyperplasia and impaired exploration patterns. Hum Mol Genet 7:999–1009.

Fukuda T, Kawano H, Ohyama K, Li H, Takeda Y, Oohira A, Kawamura K (1997) Immunohistochemical localization of neurocan and L1 in the formation of thalamocortical pathway in developing rats. J Comp Neurol 382:141–152.

Fushiki S, Schachner M (1986) Immunocytochemical localization of cell adhesion molecules L1 and N-CAM and the shared carbohydrate epitope L2 during development of the mouse neocortex. Dev Brain Res 24:153–167.

Garver TD, Ren Q, Tuvia S, Bennett V (1997) Tyrosine phosphorylation at a site highly conserved in the L1 family of cell adhesion molecules abolishes ankyrin binding and increases lateral mobility of neurofascin. J Cell Biol 137:703–714.

Grumet M (1992) Structure, expression and function of Ng-CAM, a member of the immunoglobulin superfamily involved in neuron-neuron and neuron-glia adhesion. J Neurosci Res 31:1–13.

Grumet M, Friedlander DR, Sakurai T (1996) Functions of brain chondroitin sulfate proteoglycans during development: interactions with adhesion molecules. Perspect Dev Neurobiol 3:319–330.

Heiland PC, Griffith LS, Lange R, Schachner M, Hertlein, B, Traub O, Schmitz B (1998) Tyrosine and serine phosphorylation of the neural cell adhesion molecule L1 is implicated in its oligomannosidic glycan dependent association with NCAM and neurite outgrowth. Eur J Cell Biol 75:97–106.

Hofmann MH, Bleckmann H (1999) Effect of temperature and calcium on transneuronal diffusion of DiI in fixed brain preparations. J Neurosci Meth 88:27–31.

Honig MG, Petersen GG, Rutishauser US, Camilli SJ (1998) In vitro studies of growth cone behavior support a role for fasciculation mediated by cell adhesion molecules in sensory axon guidance during development. Dev Biol 204:317–326.

Honig MG, Camilli SJ, Xue Q (2002) Effects of L1 blockade on sensory axon outgrowth and pathfinding in the chick hindlimb. Dev Biol 243:137–154.

Hortsch M (1996) The L1 families of neural cell adhesion molecules: old proteins performing new tricks. Neuron 17:587–593.

Hrynkow SH, Morest DK, Bilak M, Rutishauser U (1998) Multiple roles of neural cell adhesion molecule, neural cell adhesion molecule-polysialic acid and L1 adhesion molecules during sensory innervation of the otic epithelium in vitro. Neuroscience 87:423–437.

Jensen KF, Killackey HP (1987) Terminal arbors of axons projecting to the somatosensory cortex of the adult rat. I., The normal morphology of specific thalamocortical afferents. J Neurosci 7:3529–3543.

Kamiguchi H, Lemmon V (2000) Recycling of the cell adhesion molecule L1 in axonal growth cones. J Neurosci 20:3676–3686.

Killackey HP, Rhoades RW, Bennett-Clarke CA (1995) The formation of a cortical somatotopic map. Trends Neurosci 18:402–407.

Kunz S, Spirig M, Ginsburg C, Buchstaller A, Berger P, Lanz R, Rader C, Vogt L, Kunz B, Sonderegger P (1998) Neurite fasciculation mediated by complexes of axonin-1 and Ng cell adhesion molecule. J Cell Biol 143:1673–1690.

Lagenaur C, Lemmon V (1987) An L1-like molecule, the 8D9 antigen is a potent substrate for neurite extension. Proc Natl Acad Sci USA 84:7753–7757.

Landmesser L, Dahm L, Schultz K, Rutishauser U (1988) Distinct roles for adhesion molecules during innervation of embryonic chick muscle. Dev Biol 130:645–670.

Lemmon V, Farr KL, Lagenaur C (1989) L1-mediated axon outgrowth occurs via a homophilic binding mechanism. Neuron 2:1597–1603.

Letourneau PC (1996) The cytoskeleton in nerve growth cone motility and axonal pathfinding. Perspect Dev Neurobiol 4:111–123.

Lin CH, Thompson CA, Forscher P (1994) Cytoskeletal reorganization underlying growth cone motility. Curr Opin Neurobiol 4:640–647.

Long KE, Lemmon V (2000) Dynamic regulation of cell adhesion molecules during axon outgrowth. J Neurobiol 44:230–245.

Mason CA, Wang LC (1997) Growth cone form is behavior-specific and, consequently, position-specific along the retinal axon pathway. J Neurosci 17:1086–1100.

Mitchison T, Kirschner M (1988) Cytoskeletal dynamics and nerve growth. Neuron 1:761–772.

Molnar Z, Adams R, Blakemore C (1998) Mechanisms underlying the early establishment of thalamocortical connections in the rat. J Neurosci 18:5723–5745.

Moos M, Tacke R, Scherer H, Teplow D, Fruh K, Schachner M (1988) Neural cell adhesion molecule L1 is a member of the immunoglobulin superfamily with binding domains similar to fibronectin. Nature 334:701–703.

Needham LK, Thelen K, Maness PF (2001) Cytoplasmic domain mutations of the L1 cell adhesion molecule reduce L1-ankyrin interactions. J Neurosci 21:1490–1500.

Oster SF, Bodeker MO, He F, Sretavan DW (2003) Invariant Sema5A inhibition serves an ensheathing function during optic nerve development. Development 130: 775–784.

Polleux F, Giger RJ, Ginty DD, Kolodkin AL, Ghosh A (1998) Patterning of cortical efferent projections by semaphorin–neuropilin interactions. Science 282:1904–1906.

Raper JA (2000) Semaphorins and their receptors in vertebrates and invertebrates. Curr Opin Neurobiol 10:88–94.

Rathjen FG, Wolff JM, Frank R, Bonhoeffer F, Rutishauser U (1987) Membrane glycoproteins involved in neurite fasciculation. J Cell Biol 104:343–353.

Scotland P, Zhou D, Benveniste H, Bennett V (1998) Nervous system defects of AnkyrinB (–/–) mice suggest functional overlap between the cell adhesion molecule L1 and 440-kD AnkyrinB in premyelinated axons. J Cell Biol 143:1305–1315.

Singleton CD, Casagrande VA (1996) A reliable and sensitive method for fluorescent photoconversion. J Neurosci Methods 64:47–54.

Skaliora I, Singer W, Betz H, Pushel AW (1998) Differential patterns of semaphorin expression in the developing rat brain. Eur J Neurosci 10:1215–1229.

Suter DM, Forscher P (2000) Substrate–cytoskeletal coupling as a mechanism for the regulation of growth cone motility and guidance. J Neurobiol 44:97–113.

Suter DM, Errante LD, Belotserkovsky V, Forscher P (1998) The Ig superfamily cell adhesion molecule, apCAM, mediates growth cone steering by substrate–cytoskeletal coupling. J Cell Biol 141:227–240.

Szebenyi G, Callaway JL, Dent EW, Kalil K (1998) Interstitial branches develop from active regions of the axon demarcated by the primary growth cone during pausing behaviors. J Neurosci 18:7930–7940.

Tessier-Lavigne M, Goodman CS (1996) The molecular biology of axon guidance. Science 274:1123–1133.

Walsh FS, Doherty P (1997) Neural cell adhesion molecules of the immunoglobulin superfamily. Annu Rev Cell Dev Biol 13:425–456.

Weiland UM, Ott H, Bastmeyer M, Schaden H, Giordano S, Stuermer CA (1997) Expression of an L1-related cell adhesion molecule on developing CNS fiber tracts in zebrafish and its functional contribution to axon fasciculation. Mol Cell Neurosci 9:77–89.

Woolsey TA, Van der Loos H (1970) The structural organization of layer IV in the somatosensory region (SI) of mouse cerebral cortex. The description of a cortical field composed of discrete cytoarchitectonic units. Brain Res 17:205–242.

Xiao ZC, Revest JM, Laeng P, Rougon G, Schachner M, Montag D (1998) Defasciculation of neurites is mediated by tenascin-R and its neuronal receptor F3/11. J Neurosci Res 52:390–404.

Yamasaki M, Thompson P, Lemmon V (1997) CRASH syndrome: mutations in L1CAM correlate with severity of the disease. Neuropediatrics 28:175–178.

Yu J, Huang AS, Kolodkin AL (2000) Semaphorin-1a acts in concert with the cell adhesion molecules fasciclin II and connectin to regulate axon fasciculation in *Drosophila*. Genetics 156:723–731.

Zisch AH, Stallcup WB, Chong LD, Dahlin-Huppe K, Voshol J, Schachner M, Pasquale EB (1997) Tyrosine phosphorylation of L1 family adhesion molecules: implication of the Eph kinase Cek5. J Neurosci. Res 47:655–665.